ACS APPLIED ENERGY MATERIALS

www.acsaem.org Letter

Degrade-Repair Cycle of a Fuel-Forming Photoelectrode

Nghi P. Nguyen, Lillian K. Hensleigh, Daiki Nishiori, Edgar A. Reyes Cruz, and Gary F. Moore*

Cite This: *ACS Appl. Energy Mater.* 2022, 5, 13128−13133 Read Online

ACCESS | Metrics & More | Article Recommendations | Supporting Information

ABSTRACT: Artificial leaves that produce fuels using sunlight hold promise for sustainably powering the planet, but they require advancements in energetic efficiency, cost effectiveness, and operational durability. Herein, we showcase the application of combined surface-sensitive spectroscopic techniques to durability studies that characterize structural changes accompanying functional degradation and go beyond just observing changes in function over time. The photoelectrodes used in this work feature a polymeric surface coating functionalized with molecular complexes that catalyze the hydrogen evolution reaction. Using a polymeric layer to interface the light-harvesting component with catalytic sites enables reassembly of catalysts that detach during operation, establishing a degrade-repair cycle.

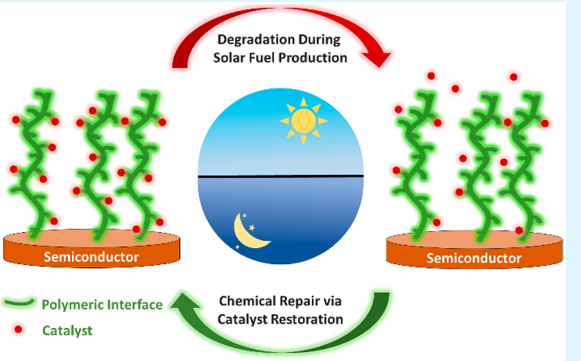

KEYWORDS: *photo-electrochemistry, hydrogen evolution reaction, polymeric coatings, molecular catalysts, degradation mechanisms, surface characterization techniques*

Artificial leaves that use sunlight for efficiently powering energetically uphill chemical transformations offer pathways to sustainably manufacturing fuels and other industrially relevant chemical products.[1−4] Efficiency, however, is not enough for large-scale, global deployment. Scalability requires the component materials are also relatively low-cost to manufacture and durable. Nature offers some design aspirations in the process of biological photosynthesis, especially as they relate to using earth-abundant, low-cost elements and achieving durability via repair rather than inherent material stability.

In this Letter, we investigate the degradation in performance and structure of a photoelectrode featuring a polymeric coating applied to a visible-light-absorbing semiconductor. The surface coating provides a molecular interface, where catalysts are assembled at specific functional-group sites along the surface-grafted coating. This model system (Co|PPy|GaP) (Figure 1a) is composed of a gallium phosphide (GaP) photocathode and a polypyridyl (PPy) surface coating that is used to assemble cobaloximes (Co), a relatively well-studied class of molecular catalysts for the hydrogen evolution reaction.[5−9] Surface-sensitive structural characterization performed prior to and following degradation in rates of fuel formation indicates that detachment of catalysts, resulting from breaking of the pyridyl nitrogen−cobalt coordination during redox cycling, is responsible for the changes in function over time. We further show the polymeric architecture can be used to reassemble catalytic components that degrade during photo-electrosynthetic fuel production. These studies demonstrate that, although coordinate bonds between a metal center and a polymeric functional group can be labile, they offer opportunities to explore the chemistry and engineering of achieving durability via repair rather than inherent material stability. In the context of producing *solar fuels*, this could involve operation by day and repair by night.

Previous work from our group describes synthetic methodologies for chemically grafting thin-film polymeric coatings onto conducting as well as semiconducting surfaces.[10−20] Overarching goals of these efforts include building protein-like, soft-material environments on solid-state electrode surfaces. This approach enables coordination of earth-abundant metal centers within the three-dimensional molecular coatings with the purpose of modulating, and ultimately controlling, the electronic and catalytic properties of the overall assembly. The grafting procedures leverage the UV-induced surface-attachment and polymerization chemistry of alkenes[8,21−24] and provide model assemblies for studying the effects of polymeric encapsulation on electrocatalytic[11,18,19] as well as photo-electrosynthetic[10,12−17,20] performance. Our previous work demonstrates (1) the grafting method can be utilized on a range of oxide-terminated surfaces,[10−20] (2) the polymer grafting is not limited to a specific crystal-face orientation,[10,11] (3) the film thickness of the grafts—ranging from a few nanometers to submicrons—is sensitive to the reaction solvent

Received: July 25, 2022
Accepted: October 3, 2022
Published: November 15, 2022

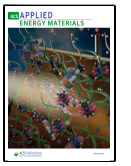

https://doi.org/10.1021/acsaem.2c02367
ACS Appl. Energy Mater. 2022, 5, 13128−13133

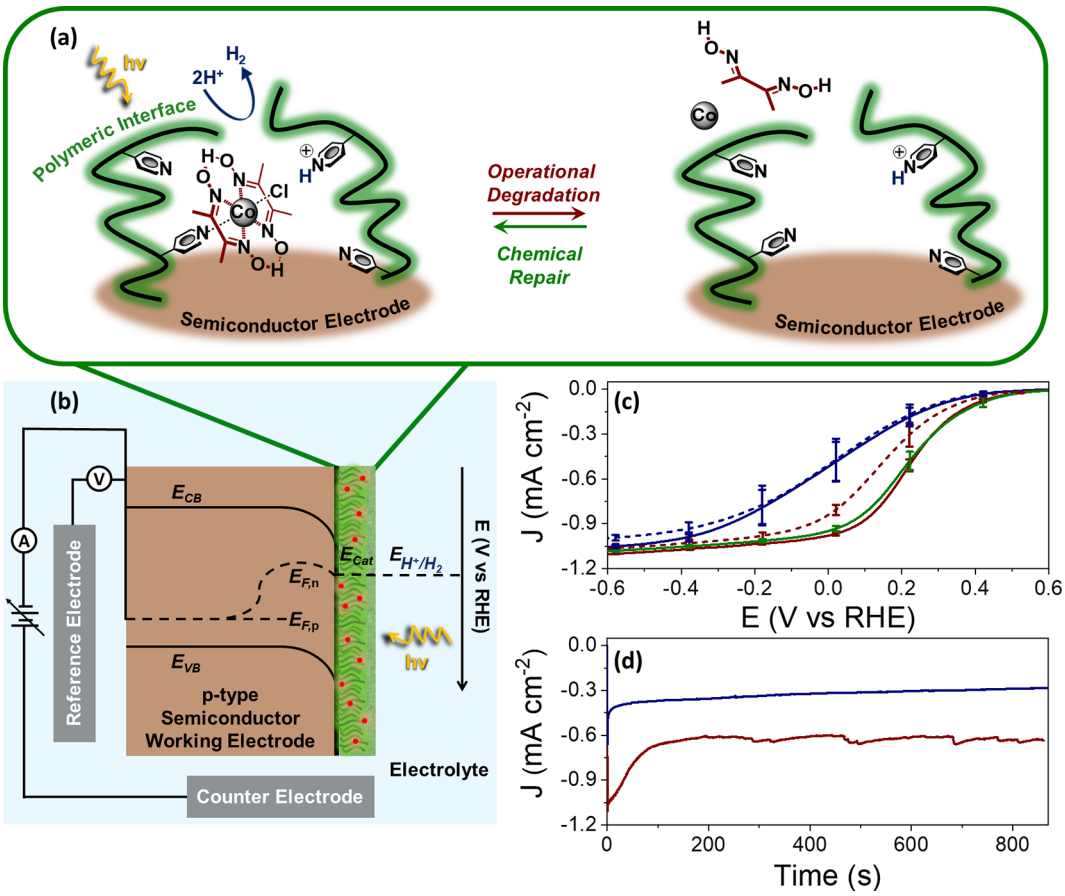

Figure 1. (a) Schematic representation of the ColPPylGaP degrade-repair cycle. (b) Schematic illustration of the three-electrode assembly featuring a molecular-modified p-type semiconductor working electrode under steady-state illumination at open-circuit conditions. E_{CB} is the conduction band-edge potential, E_{VB} is the valence band-edge potential, $E_{F,n}$ is the electron quasi-Fermi level, $E_{F,p}$ is the hole quasi-Fermi level, E_{cat} is the catalyst potential, E_{H^+/H_2} is the thermodynamic hydrogen potential, and V_{ph} is the photovoltage. (c) Voltammograms recorded using ColPPylGaP electrodes prior to (red) and following (red dash) degradation via controlled-potential electrolysis at 0 V vs RHE (see Figure 1d and related caption) as well as subsequent repair via wet-chemical processing (green). Voltammograms recorded using PPylGaP electrodes prior to (blue) and following (blue dash) the same controlled-potential electrolysis experiments are included for comparison. All voltammograms were recorded in 0.1 M phosphate buffer (pH 7) solution, at a scan rate of 100 mV s^{-1}, and under 100 mW cm^{-2} illumination. (d) Current density vs time plots obtained via 15 min of controlled-potential electrolysis at 0 V vs RHE using either ColPPylGaP (red) or PPylGaP (blue) electrodes in 0.1 M phosphate buffer (pH 7) and under 100 mW cm^{-2} illumination.

conditions, illumination conditions, and the chemical nature of the underpinning support (including doping levels in the case of semiconductors),[10−20] (4) the polymeric functional groups can be modified to control the (photo)electrosynthetic activity of the overall assembly,[12] (5) synthetic manipulation of the attached catalysts' ligand environment at the molecular level affects the photo-electrochemical response observed at the construct level,[13] and (6) the polymeric immobilization strategy is not limited to a single class of molecular catalysts and, thus, provides a modular-assembly approach.[14,15]

To facilitate comparisons between results obtained via grazing angle attenuated total reflection Fourier transform infrared (GATR-FTIR) spectroscopy—which probes up to micrometers in depth—and X-ray photoelectron (XP) spectroscopy—which probes only a few nanometers in depth—the polypyridyl-modified samples (PPylGaP) described in this Letter were intentionally prepared with a relatively thin PPy coating (~2.31 ± 0.01 nm, as determined by spectroscopic ellipsometry). Following postsynthetic modification of the PPylGaP samples, via wet chemical processing with a 1.0 mM methanolic solution of the cobalt-containing precursor Co(dmgH$_2$)(dmgH)Cl$_2$ (dmgH = dimethylglyoximate monoanion and dmgH$_2$ = dimethylglyoxime, see experimental methods and Scheme S1 of the Supporting Information for further details), 31 ± 1% of the pyridyl groups on the surface graft are coordinated to a cobaloxime cobalt center (as determined via XP spectroscopy analysis, see Table S3). This yields a per-geometric-area cobaloxime loading of 1.75 ± 0.06 nmol cm^{-2} with a film thickness (as determined by spectroscopic ellipsometry) that increases to 5.16 ± 0.01 nm (Figure S6). These film thickness and loading conditions were also selected to facilitate structural characterization, performed prior to and following photo-electrosynthetic operation with minimized experimental times and, thus, reduced risks of contaminating the samples. In addition, a customized photo-electrochemical cell that makes electrical contact with the unfunctionalized face of the semiconductors and facilitates relatively rapid loading and unloading of electrode samples to and from the cell was used in these experiments (Figure S1).

The photo-electrosynthetic performance of the GaP, PPylGaP, and ColPPylGaP electrode assemblies was assessed via a combination of three-electrode voltammetry (Figure 1c and

https://doi.org/10.1021/acsaem.2c02367
ACS Appl. Energy Mater. 2022, 5, 13128−13133

Figure S30) and controlled-potential electrolysis (Figure 1d and Figure S31) using aqueous solutions buffered at pH 7 (0.1 M phosphate buffer) and 100 mW cm^{-2} simulated-solar-illumination (Figure S34). Results from these experiments, including the short-circuit current densities (J_{SC}), open-circuit voltages (V_{OC}), and fill factors (*ff*), measured prior to and following 15 min of controlled-potential electrolysis at 0 V versus the reversible hydrogen electrode (RHE) potential, are summarized in Table S4. Following the initial voltammetry and controlled-potential electrolysis experiments recorded using the CoIPPy|GaP working electrodes, the J_{SC} decreased from 0.98 ± 0.01 to 0.84 ± 0.04 mA cm^{-2} (corresponding to a 14 ± 3% decrease in activity). Likewise, the V_{OC} decreased from 0.718 ± 0.005 to 0.65 ± 0.03 V vs RHE (corresponding to a 10 ± 4% decrease), and the *ff* decreased from 0.17 ± 0.01 to 0.14 ± 0.02 (corresponding to a 20 ± 4% decrease). These electrodes also showed a decline in the steady-state photocurrent recorded during the 15 min of controlled-potential electrolysis, from an initial value of 1.05 ± 0.03 mA cm^{-2} to a final value of 0.63 ± 0.07 mA cm^{-2} (an overall 39 ± 6% decrease). Results from control experiments, performed using GaP and PPy|GaP as the working electrodes, are included as Supporting Information (Table S4).

Spectroscopic measurements, including GATR-FTIR spectroscopy and XP spectroscopy, were performed prior to and following the series of voltammetry and controlled-potential electrolysis experiments. GATR-FTIR spectroscopy was used to monitor the relative intensity of absorption bands on the surfaces that are associated with vibrational modes of free-base pyridyl groups versus pyridyl groups coordinated to cobaloxime units (Figure 2 and Figure S13). In particular, the relative intensity ratios of peaks assigned to the NO^- stretching mode

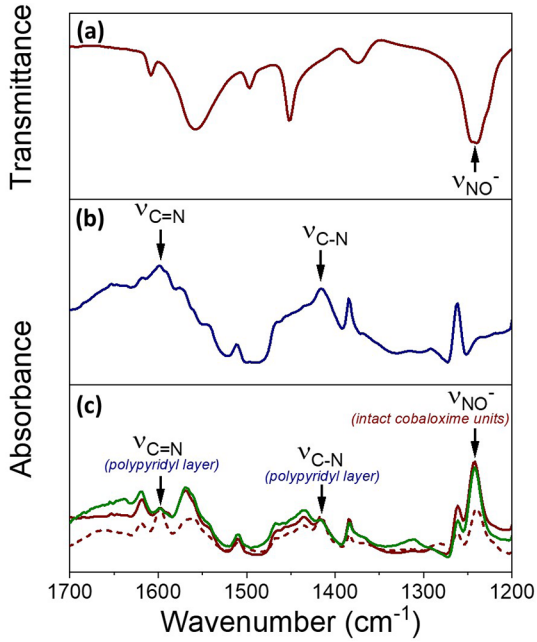

Figure 2. (a) FTIR transmission spectrum of the model cobaloxime complex, $Co(dmgH)_2PyCl$, in KBr (red solid). (b) GATR-FTIR spectrum of PPy|GaP recorded using *initial* sample (blue solid). (c) GATR-FTIR spectra of CoIPPy|GaP samples recorded using *initial* (red solid), *postdegrade* (see Figure 1d and related caption) (red dash), and *postrepair* (green solid) samples. All spectra are normalized to the absorbance peak at 1600 cm^{-1}.

of intact cobaloximes (1240 cm^{-1})[25] and those assigned to either the C═N (1600 cm^{-1}) or C−N (1417 cm^{-1}) vibrations of the polypyridyl layer were compared before and after photoelectrosynthetic operation.[26] Comparing relative intensity ratios, rather than absolute intensities, avoids sample-to-sample discrepancies in signal intensities arising from varying contact between the GaP semiconductor samples and the attenuated total reflectance crystal of the GATR-FTIR unit. These results are summarized in Table S1 and indicate a 74 ± 2% reduction of the cobaloxime loadings following the series of voltammetry and controlled-potential experiments (Table S1).

XP spectroscopy yields additional insights on the structural differences of the electrode coatings prior to and following photo-electrosynthetic operation. As compared with the N 1s core-level XP spectra of PPy|GaP surfaces, which display a single N 1s feature assigned to pyridyl nitrogens of the surface graft,[12] the N 1s core-level XP spectra of CoIPPy|GaP surfaces are more complex, with overlapping spectral features that are fit using three components (Figure 3). These include a component centered at 398.0 eV assigned to free-base pyridyl nitrogens (abbreviated as PyN), a component centered at 399.5 eV assigned to glyoximate nitrogens of the cobaloxime ligands (abbreviated as GlyN), and a component centered at 400.5 eV assigned to pyridyl nitrogens coordinated to cobalt centers of cobaloximes (abbreviated as PyN-Co).

Comparisons of the PyN-Co/PyN signal intensity ratios, determined prior to and following photo-electrosynthetic operation, indicate a 79 ± 1% reduction of the cobaloxime surface loadings following the series of voltammetry and controlled-potential experiments (Table S2). Further structural information is provided by comparing the total Co 2p/N 1s spectral intensity ratios, which indicate an 84 ± 2% reduction of the cobaloxime surface loadings following the series of photo-electrochemical experiments (Table S3). Although there is a significant decrease in the Co 2p core-level signal intensity following photo-electrosynthetic operation, the Co 2p features maintain a 2:1 branching ratio with a 15.0 eV peak separation. There are also no detectable peaks corresponding to the presence of cobalt oxide or metallic cobalt (Figure S29), indicating the remnant cobalt signals are associated with intact cobaloxime complexes.[8,27]

Given our spectroscopic measurements indicating (1) the degradation of fuel-production rates during photo-electrochemical operation is accompanied by a loss of chemically grafted cobaloxime units and (2) there is a persistence of spectroscopic markers associated with the PPy graft following this loss of cobaloximes, we explored the possibility of restoring the fuel-production activity by chemically repairing/restoring cobaloximes onto the surface-grafted polymer. Following chemical reprocessing of the cobaloxime-depleted electrodes via treatment with a 1.0 mM methanolic solution of $Co(dmgH_2)(dmgH)Cl_2$ (see experimental methods and Scheme S1 of the Supporting Information for further details), the photo-electrosynthetic performance metrics of the electrodes are restored to their original values, within the error of the measurements (see Figure 1c and Table S4).

Structural characterization of these chemically repaired electrodes is also consistent with successful restoration of the cobaloxime loadings. In particular, signal-intensity analyses using GATR-FTIR data, deconvolution of N 1s core level XP spectra, and comparison of Co 2p/N 1s spectral intensity ratios all indicate nearly quantitative restoration of the initial cobaloxime loadings recorded prior to any degradation

https://doi.org/10.1021/acsaem.2c02367
ACS Appl. Energy Mater. 2022, 5, 13128−13133

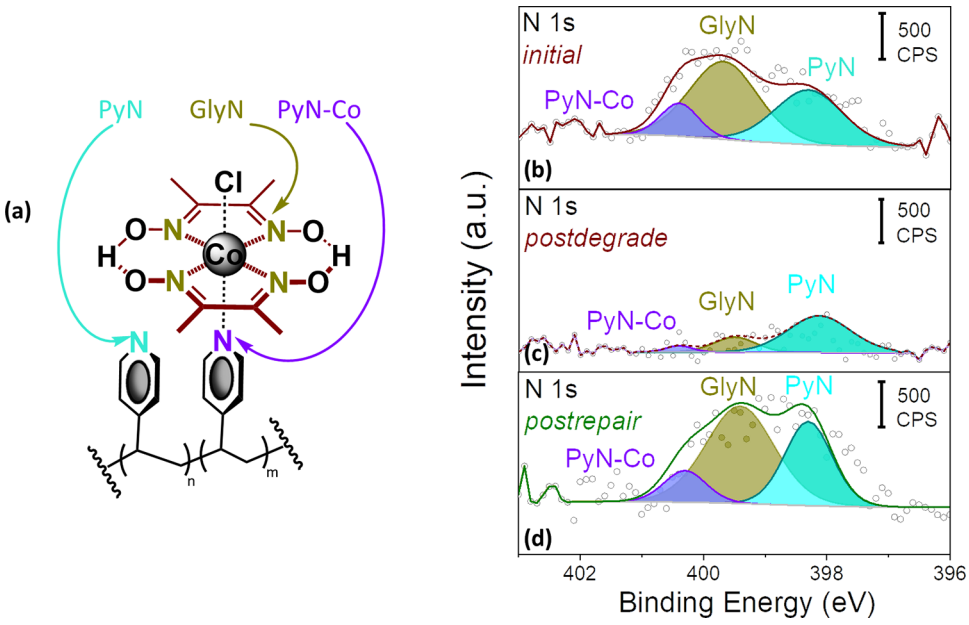

Figure 3. (a) Structure of the pyridyl and cobaloxime units of ColPPylGaP indicating the PyN, GlyN, and PyN-Co nitrogen sites. (b–d) N 1s core-level XP spectra of ColPPylGaP recorded using (b) *initial*, (c) *postdegrade* (see Figure 1d and related caption), and (d) *postrepair* samples. Solid lines represent the background (gray) and indicated components (cyan for remnant pyridyl nitrogens (PyN), yellow for glyoximate nitrogens bound to cobalt centers (GlyN), and purple for pyridyl nitrogens bound to cobaloximes (PyN-Co)).

(yielding values of 96 ± 3%, 95 ± 3%, and 95 ± 4% restoration of the initial cobalt loadings for the three types of measurements, respectively) (Tables 1 and S1–S3). Product

Table 1. Per-Geometric-Area Cobaloxime Loadings[a]

sample	cobaloxime loading (nmol Co cm^{-2})[a]
ColPPylGaP (*initial*)	0.82 ± 0.01
ColPPylGaP (*postdegrade*)	0.172 ± 0.009
ColPPylGaP (*postrepair*)	0.78 ± 0.02

[a]As determined via a combination of ellipsometry and XP spectroscopy (see experimental in Supporting Information for further details).

detection via gas chromatography experiments performed using *initial*, *postdegrade*, and *postrepair* electrodes confirms hydrogen production in the case of all samples (Figures S2–S5). Further, as demonstrated by performing three successive degrade-repair cycles (Figure S33), the restoration of photoelectrochemical activity following chemical repair is not limited to a single cycle.

Considering the results described in this Letter (obtained using a model polypyridyl-cobaloxime-modified semiconductor assembly) and those of previous reports on the electrocatalytic performance and operational mechanisms of homogeneous cobaloxime catalysts,[5–9,28,29] we postulate the loss of cobaloximes during photo-electrosynthetic operation is, in part, triggered by redox cycling and an associated breaking of pyridyl nitrogen–cobalt bonds during reduction of the cobalt centers from their Co^{II} to Co^{I} oxidation states. Although a redundancy of ligand sites and confinement effects associated with polymeric coatings appear to impart increased chemical stability of the cobaloxime units as compared to their homogeneous counterparts,[11] fragments of the cobaloximes leach from the surface-immobilized polymer during photo-electrosynthetic operation. By comparison, related studies using porphyrins grafted to GaP surfaces via an intervening PPy coating,[16–18] or via more covalent-based attachment strategies,[14,15,18] show enhanced durability as measured by the decreases in their fuel-production activities over time. These results indicate the selection of catalyst type, the chemical nature of their attachment, their degree of solubility in the electrolyte solution, and the thickness of any immobilizing polymer coatings all influence the robustness of the attachment chemistry.

It has not escaped our attention that the loss of photo-electrosynthetic activities described in this Letter, as observed during the 15 min of controlled-potential electrolysis experiments using ColPPylGaP working electrodes intentionally prepared with a relatively thin (~2.31 ± 0.01 nm) PPy coating, is not linear (see Figure 1d). In these experiments, there is an initial, more rapid loss of activity that occurs during the first ~150 s (with a 39 ± 6% decrease of current density from 1.05 ± 0.03 to 0.64 ± 0.06 mA cm^{-2}). This is followed by a relatively more stable phase (with a 2 ± 14% change in the current density to a value of 0.63 ± 0.07 mA cm^{-2} at the end of the overall 15 min experiment). We speculate the upfront loss in activity is a consequence of catalyst detachment at points loosely associated with the polymeric coating and/or at sites more directly exposed to the bulk electrolyte.

The relatively larger percent loss of cobaloximes following operational degradation as compared to the percent loss in fuel-production metrics implies not all of the lost Co complexes contributed, or contributed equally, to the initial photo-electrosynthetic performance.[11,17] In addition to degradation of cobaloxime catalysts, we cannot rule out that some fraction of the performance loss is due to damage induced at the underlying semiconductor (e.g., formation of surface oxides, see Figure S12) or intervening polymeric scaffold. Nonetheless, the nearly complete restoration of activity following repair of the electrodes by restoring the loading of cobaloximes indicates the overall performance loss is largely

https://doi.org/10.1021/acsaem.2c02367
ACS Appl. Energy Mater. 2022, 5, 13128–13133

(i.e., within the error of the measurements reported in this Letter) associated with degradation of cobaloxime sites.

In summary, the polypyridyl-cobaloxime-modified semiconductors used in these experiments are purposefully designed for fundamental studies aimed at better understanding the structure−function relationships of hybrid interfaces involving hard- and soft-material components. These assemblies afford opportunities to study their photoelectrosynthetic performance, degradation, and accompanying structural changes. Consistent with the proposed mechanism of the activity loss being linked to structural degradation at cobaloxime catalyst sites, we show the activity can be restored by chemically repairing the cobaloximes. Although demonstration of a degrade-repair cycle is a promising feature in the context of developing schemes to generate solar fuels by day coupled with repair at night, further advancements are required for commercial-based applications. In general, designing, interfacing, and characterizing combinations of (semi)-conducting and catalytic materials to effectively power chemical transformations remain outstanding challenges. Addressing this will likely require development of new materials and material interfaces, improved models for better understanding how charge carriers move across these hybrid assemblies, and standardized techniques for benchmarking their overall performance.[30]

■ ASSOCIATED CONTENT

Supporting Information

The Supporting Information is available free of charge at https://pubs.acs.org/doi/10.1021/acsaem.2c02367.

Experimental methods, molecular structures, a synthetic scheme, further information on the workflow and processing of samples, additional experimental data and references (PDF)

■ AUTHOR INFORMATION

Corresponding Author

Gary F. Moore − *School of Molecular Sciences and the Biodesign Institute Center for Applied Structural Discovery, Arizona State University, Tempe, Arizona 85287-1604, United States;* orcid.org/0000-0003-3369-9308; Email: gfmoore@asu.edu

Authors

Nghi P. Nguyen − *School of Molecular Sciences and the Biodesign Institute Center for Applied Structural Discovery, Arizona State University, Tempe, Arizona 85287-1604, United States;* orcid.org/0000-0002-8970-3372

Lillian K. Hensleigh − *School of Molecular Sciences and the Biodesign Institute Center for Applied Structural Discovery, Arizona State University, Tempe, Arizona 85287-1604, United States*

Daiki Nishiori − *School of Molecular Sciences and the Biodesign Institute Center for Applied Structural Discovery, Arizona State University, Tempe, Arizona 85287-1604, United States;* orcid.org/0000-0002-4707-0896

Edgar A. Reyes Cruz − *School of Molecular Sciences and the Biodesign Institute Center for Applied Structural Discovery, Arizona State University, Tempe, Arizona 85287-1604, United States;* orcid.org/0000-0001-7307-7613

Complete contact information is available at: https://pubs.acs.org/10.1021/acsaem.2c02367

Author Contributions

The manuscript was written through contributions of all authors. All authors have given approval to the final version of the manuscript.

Notes

The authors declare no competing financial interest.

■ ACKNOWLEDGMENTS

This material is based upon work supported by the National Science Foundation under Early Career Award 1653982 (polymeric surface chemistry) and by the U.S. Department of Energy, Office of Science, Office of Basic Energy Sciences, under Early Career Award DE-SC0021186 (degradation kinetics and durability studies). G.F.M. acknowledges support from the Camille Dreyfus Teacher-Scholar Awards Program. N.P.N. acknowledges support from a Completion Fellowship provided by the Arizona State University Graduate College. The authors gratefully acknowledge D. Convey in the Goldwater Materials Science Facility at Arizona State University for assistance with ellipsometry measurements and T. Karcher in the Eyring Materials Center at Arizona State University for assistance with XP spectroscopy data collection.

■ REFERENCES

(1) Faunce, T. A.; Lubitz, W.; Rutherford, A. W.; MacFarlane, D.; Moore, G. F.; Yang, P.; Nocera, D. G.; Moore, T. A.; Gregory, D. H.; Fukuzumi, S.; Yoon, K. B.; Armstrong, F. A.; Wasielewski, M. R.; Styring, S. Energy and environment policy case for a global project on artificial photosynthesis. *Energy Environ. Sci.* **2013**, *6*, 695−698.

(2) Ardo, S.; Fernandez Rivas, D. F.; Modestino, M. A.; Schulze Greiving, V. S.; Abdi, F. F.; Alarcon Llado, E. A.; Artero, V.; Ayers, K.; Battaglia, C.; Becker, J.-P.; Bederak, D.; Berger, A.; Buda, F.; Chinello, E.; Dam, B.; Di Palma, V.; Edvinsson, T.; Fujii, K.; Gardeniers, H.; Geerlings, H.; H Hashemi, S. M.; Haussener, S.; Houle, F.; Huskens, J.; James, B. D.; Konrad, K.; Kudo, A.; Kunturu, P. P.; Lohse, D.; Mei, B.; Miller, E. L.; Moore, G. F.; Muller, J.; Orchard, K. L.; Rosser, T. E.; Saadi, F. H.; Schüttauf, J.-W.; Seger, B.; Sheehan, S. W.; Smith, W. A.; Spurgeon, J.; Tang, M. H.; van de Krol, R.; Vesborg, P. C. K.; Westerik, P. Pathways to Electrochemical Solar-Hydrogen Technologies. *Energy Environ. Sci.* **2018**, *11*, 2768−2783.

(3) Wadsworth, B. L.; Khusnutdinova, D.; Moore, G. F. Polymeric coatings for applications in electrocatalytic and photo-electrosynthetic fuel production. *J. Mater. Chem. A* **2018**, *6*, 21654−21665.

(4) Reyes Cruz, E. A.; Nishiori, D.; Wadsworth, B. L.; Nguyen, N. P.; Hensleigh, L. K.; Khusnutdinova, D.; Beiler, A. M.; Moore, G. F. Molecular-Modified Photocathodes for Applications in Artificial Photosynthesis and Solar-to-Fuel Technologies. *Chem. Rev.* **2022**, DOI: 10.1021/acs.chemrev.2c00200.

(5) Connolly, P.; Espenson, J. H. Cobalt-catalyzed evolution of molecular hydrogen. *Inorg. Chem.* **1986**, *25*, 2684−2688.

(6) Razavet, M.; Artero, V.; Fontecave, M. Proton Electroreduction Catalyzed by Cobaloximes: Functional Models for Hydrogenases. *Inorg. Chem.* **2005**, *44*, 4786−4795.

(7) Hu, X. L.; Cossairt, B. M.; Brunschwig, B. S.; Lewis, N. S.; Peters, J. C. Electrocatalytic hydrogen evolution by cobalt difluoroboryl-diglyoximate complexes. *Chem. Commun.* **2005**, *37*, 4723−4725.

(8) Krawicz, A.; Yang, J.; Anzenberg, E.; Yano, J.; Sharp, I. D.; Moore, G. F. Photofunctional Construct That Interfaces Molecular Cobalt-Based Catalysts for H_2 Production to a Visible-Light-Absorbing Semiconductor. *J. Am. Chem. Soc.* **2013**, *135*, 11861−11868.

(9) Dempsey, J. L.; Brunschwig, B. S.; Winkler, J. R.; Gray, H. B. Hydrogen Evolution Catalyzed by Cobaloximes. *Acc. Chem. Res.* **2009**, *42*, 1995−2004.

(10) Beiler, A. M.; Khusnutdinova, D.; Jacob, S. I.; Moore, G. F. Solar Hydrogen Production Using Molecular Catalysts Immobilized on Gallium Phosphide (111)A and (111)B Polymer-Modified Photocathodes. *ACS Appl. Mater. Interfaces* **2016**, *8*, 10038−10047.
(11) Wadsworth, B. L.; Beiler, A. M.; Khusnutdinova, D.; Jacob, S. I.; Moore, G. F. Electrocatalytic and Optical Properties of Cobaloxime Catalysts Immobilized at a Surface-Grafted Polymer Interface. *ACS Catal.* **2016**, *6*, 8048−8057.
(12) Beiler, A. M.; Khusnutdinova, D.; Jacob, S. I.; Moore, G. F. Chemistry at the Interface: Polymer-Functionalized GaP Semiconductors for Solar Hydrogen Production. *Ind. Eng. Chem. Res.* **2016**, *55*, 5306−5314.
(13) Cedeno, D.; Krawicz, A.; Doak, P.; Yu, M.; Neaton, J. B.; Moore, G. F. A Noble-Metal-Free Hydrogen Evolution Catalyst Grafted to Visible Light-Absorbing Semiconductors. *J. Phys. Chem. Lett.* **2014**, *5*, 3222−3226.
(14) Khusnutdinova, D.; Beiler, A. M.; Wadsworth, B. L.; Jacob, S. I.; Moore, G. F. Metalloporphyrin-modified semiconductors for solar fuel production. *Chem. Sci.* **2017**, *8*, 253−259.
(15) Nishiori, D.; Wadsworth, B. L.; Reyes Cruz, E. A.; Nguyen, N. P.; Hensleigh, L. K.; Karcher, T.; Moore, G. F. Photoelectrochemistry of metalloporphyrin-modified GaP semiconductors. *Photosynth Res.* **2021**, DOI: 10.1007/s11120-021-00834-2.
(16) Beiler, A. M.; Khusnutdinova, D.; Wadsworth, B. L.; Moore, G. F. Cobalt Porphyrin-Polypyridyl Surface Coatings for Photoelectrosynthetic Hydrogen Production. *Inorg. Chem.* **2017**, *56*, 12178−12185.
(17) Wadsworth, B. L.; Beiler, A. M.; Khusnutdinova, D.; Reyes Cruz, E. A.; Moore, G. F. Interplay between Light Flux, Quantum Efficiency, and Turnover Frequency in Molecular-Modified Photoelectrosynthetic Assemblies. *J. Am. Chem. Soc.* **2019**, *141*, 15932−15941.
(18) Wadsworth, B. L.; Khusnutdinova, D.; Urbine, J. M.; Reyes, A. S.; Moore, G. F. Expanding the Redox Range of Surface-Immobilized Metallocomplexes Using Molecular Interfaces. *ACS Appl. Mater. Interfaces* **2020**, *12*, 3903−3911.
(19) Wadsworth, B. L.; Nishiori, D.; Nguyen, N. P.; Reyes Cruz, E. A.; Moore, G. F. Electrochemistry of Polymeric Cobaloxime-Containing Assemblies in Organic and Aqueous Solvents. *ECS J. Solid State Sci. Technol.* **2020**, *9*, 061018.
(20) Nguyen, N. P.; Wadsworth, B. L.; Nishiori, D.; Reyes Cruz, E. A.; Moore, G. F. Understanding and Controlling the Performance-Limiting Steps of Catalyst-Modified Semiconductors. *J. Phys. Chem. Lett.* **2021**, *12*, 199−203.
(21) Steenackers, M.; Küller, A.; Stoycheva, S.; Grunze, M.; Jordan, R. Structured and Gradient Polymer Brushes from Biphenylthiol Self-Assembled Monolayers by Self-Initiated Photografting and Photopolymerization (SIPGP). *Langmuir* **2009**, *25*, 2225−2231.
(22) Wang, X.; Ruther, R. E.; Streifer, J. A.; Hamers, R. J. UV-Induced Grafting of Alkenes to Silicon Surfaces: Photoemission versus Excitons. *J. Am. Chem. Soc.* **2010**, *132*, 4048−4049.
(23) Seifert, M.; Koch, A. H. R.; Deubel, F.; Simmet, T.; Hess, L. H.; Stutzmann, M.; Jordan, R.; Garrido, J. A.; Sharp, I. D. Functional Polymer Brushes on Hydrogenated Graphene. *Chem. Mater.* **2013**, *25*, 466−470.
(24) Moore, G. F.; Sharp, I. D. A Noble-Metal-Free Hydrogen Evolution Catalyst Grafted to Visible Light-Absorbing Semiconductors. *J. Phys. Chem. Lett.* **2013**, *4*, 568−572.
(25) Yamazaki, N.; Hohokabe, Y. Studies on Cobaloxime Compounds. I. Synthesis of Various Cobaloximes and Investigation on Their Infrared and Far-Infrared Spectra. *Bull. Chem. Soc. Jpn.* **1971**, *44*, 63−69.
(26) Panov, V. P.; Kazarin, L. A.; Dubrovin, V. I.; Gusev, V. V.; Kirsh, Y. E. Infrared spectra of atactic poly-4-vinylpyridine. *J. Appl. Spectrosc.* **1974**, *21*, 1504−1510.
(27) Chuang, T. J.; Brundle, C. R.; Rice, D. W. Interpretation of the x-ray photoemission spectra of cobalt oxides and cobalt oxide surfaces. *Surf. Sci.* **1976**, *59*, 413−429.
(28) Muckerman, J. T.; Fujita, E. Theoretical studies of the mechanism of catalytic hydrogen production by a cobaloxime. *Chem. Commun.* **2011**, *47*, 12456−12458.
(29) Veldkamp, B. S.; Han, W. S.; Dyar, S. M.; Eaton, S. W.; Ratner, M. A.; Wasielewski, M. R. Photoinitiated multi-step charge separation and ultrafast charge transfer induced dissociation in a pyridyl-linked photosensitizer-cobaloxime assembly. *Energy Environ. Sci.* **2013**, *6*, 1917−1928.
(30) Nishiori, D.; Wadsworth, B. L.; Moore, G. F. Parallels between enzyme catalysis, electrocatalysis, and photoelectrosynthesis. *Chem. Catal.* **2021**, *1*, 978−996.

https://doi.org/10.1021/acsaem.2c02367
ACS Appl. Energy Mater. 2022, 5, 13128−13133